Photonic Sensors (2013) Vol. 3, No. 2: 137–143

DOI: 10.1007/s13320-012-0061-8 **Photonic Sensors**

Regular

Analog Processing Based Vibration Measurement Technique Using Michelson Interferometer

Babar HUSSAIN, Mushtaq AHMED, Ghazanfar HUSSAIN, Muhammad SALEEM, and Muhammad NAWAZ

National Institute of Lasers and Optronics, 45650, Islamabad, Pakistan

*Corresponding author: Babar HUSSAIN Email: babarhussain2002@hotmail.com

Abstract: A Michelson interferometer based sensor, to monitor the displacement and vibration of a surface, is presented. The interference signals detected in quadrature are processed using analog electronics to find the direction of the motion of a vibrating surface in real-time. The complete instrumentation and signal processing are implemented for the interpretation of the amplitude as well as positive and negative excursion of the vibration cycles. This new technique is simpler as compared to the techniques commonly used in the interferometer based vibration sensors. Using this technique, we have measured mechanical vibrations having a magnitude of the order of nanometers and frequency in the range of 50 Hz to 500 Hz. By making small changes in the electronic circuit, the technique can be implemented for the extended range of the vibration frequencies and amplitude.

Keywords: Vibration sensor, displacement sensor, Michelson interferometer, direction detection, analog processing

1. Introduction

Mechanical vibrations of small or large amplitudes are required to be monitored precisely in sophisticated systems. Various interferometric techniques to measure the vibration and displacement of a surface have been reported. These techniques are based on holographic interferometry [1], speckle interferometry [2], shadow Moiré method [3], and classical interferometry [4–13]. The basic principle in most of these techniques is same, that is two coherent beams from a single source are interfered to form interference fringes. One of the beams is used as a reference beam while the other one is signal beam that is reflected from the vibrating surface under consideration. The displacement of the surface is translated into the optical pathlength change that in turn is transformed to the fringe movement. After processing the fringe movement, the information about the mechanical movement is obtained. Many other parameters are also measured using the change in the pathlength of the interferometer, for example, strain/pressure, temperature etc. [14, 15].

All the methods mentioned above, except the classical interferometry, have a common limitation that the vibrating surface under study should be fixed at some point for reference. Also, these techniques are unable to detect the direction of the motion. Classical interferometry, on the other hand, can be used for the detection of the real-time displacement and the vibration of a body. The optical signal achieved can also be used to determine the direction of the displacement of the vibrating surface in real time. The vibration of the amplitude less than 1nm and the displacement of the order of meters can be measured.

Previously, a novel technique was presented to

Received: 31 March 2012 / Revised version: 23 May 2012

find the direction of the motion along with the amplitude of the vibration [5, 6, 8]. The technique was based on the use of two photodiodes that detected complementary fringes at two ports of a beam splitter. The two signals from the photodiodes, after amplification, were acquired to perform digital processing for the measurement of the amplitude as well as the direction of the motion. We reported a technique that measured the displacement and its direction using spatial phase quadrature in the analog electronics domain. The system would be portable and applicable to detect vibrations in the field like vibration measurement of bridges.

Laser Doppler vibrometer (LDV) systems are commercially available to measure vibration at one point, over a surface or in a 3-dimentional object and their cost and complexity vary accordingly. Mostly, there are two interferometer setups (heterodyne and homodyne) used in LDV systems to measure the frequency and amplitude of the vibration. In the heterodyne interferometer based systems, a Bragg-cell is used to produce a frequency shift in the reference laser beam [16]. An extra circuit is required to operate the Bragg-cell. Our technique does not need the Bragg-cell and the circuit required to operate the Bragg-cell, therefore, our technique is simpler and less expensive. Secondly, in our technique, less effort is required for digital processing since most of the processing is performed through the analog circuit. In homodyne interferometer based systems, additional components, a $\lambda/8$ plate and a polarizing beamsplitter, are used to introduce the directional sensitivity so that the frequency and amplitude of the vibration can be calculated. Our technique has worth because it eliminates the need for the $\lambda/8$ plate and polarizing beamsplitter.

2. Description

We have experimentally demonstrated a technique in which two photodiodes are used to detect a fringe pattern at spatial quadrature in real time without using an extra beam splitter and transmission gratings. Our method processes the signals in the analog electronics regime to detect the movement and its direction using the differentiator, multiplier, and integrator. The output of the circuit follows the differential of the movement e.g. it reverses its polarity after each half cycle of the vibration when the vibrating surface changes its direction. Our technique makes the system smarter, faster, and less expensive. The frequency of the vibration can be measured with more convenience, even without using a computer.

The schematic of the setup used for the experiments is shown in Fig. 1. The mirror M_1 is slightly tilted to form spatially linear fringes [shown in (4)], and M_2 is the reflecting vibrating surface that moves in the direction a or b. A mirror can also be mounted on the vibrating surface for this purpose. A diverging lens can be used to achieve the fringe pattern with a larger size. The larger size of the fringe pattern helps to detect the signals using two photodiodes (PD_1 and PD_2) placed in spatial quadrature. Figure 2 shows that the two photodiodes are placed at a phase separation of $\pi/2$ with respect to the intensity profile of the fringe pattern. Let us assume that L_1 and L_2 are the optical path differences (OPDs) corresponding to PD_1 and PD_2, respectively. The phase of the interference signal detected by PD_1 can be expressed as

$$\alpha(t)=\frac{2\pi}{\lambda}L_1(t) \tag{1}$$

where the constant phase difference between the outputs of the two photodiodes is

$$\varphi=\frac{2\pi}{\lambda}(L_2-L_1). \tag{2}$$

In our technique, the two photodiodes are adjusted precisely using a mechanical arrangement such as

$$\varphi\cong\pm(\pi/2+n\pi) \qquad n=0,1,2,.... \tag{3}$$

If the fringe spacing (FS) is too small, higher values of n can be selected to adjust the photodiodes. However, as the fringe spacing is reduced, a correspondingly smaller area photodiode is required.

The fringe spacing is given by

$$FS = \frac{\lambda}{2\sin(\theta/2)} \times F \tag{4}$$

where λ is the wavelength of light, θ is the angle between two interfering beams, and F is the factor by which the fringe pattern spreads out depending on the focal length of the lens or a lens system and the distance of photodiodes from the lens. The angle between the two interfering beams can be controlled by the tilt of the mirror M_1. The distance between PD_1 and PD_2 is adjusted by moving one of the photodiodes precisely using a linear stage while observing their outputs on the oscilloscope. When the spatial phase difference between them becomes about $\pi/2$, the photodiodes are fixed there. The accuracy of the distance between PD_1 and PD_2 should be ±0.5 mm in our case. This accuracy depends on the tolerable error in phase difference between outputs of the photodiodes which in turn depends on the circuit design. When the fringes move due to the vibration, the relative phase between the two output signals will be either $+\pi/2$ or $-\pi/2$ depending on the placement of the photodiodes.

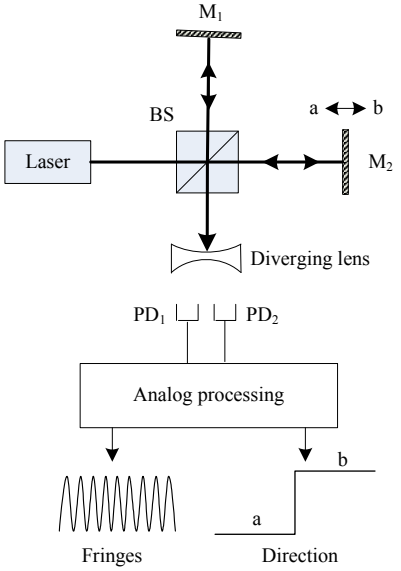

Fig. 1 Experimental arrangement for vibration/displacement measurement (BS: beam splitter; M_1 and M_2: mirrors; PD_1 and PD_2: photodiodes).

We have performed the experiments with a 1-mW He-Ne laser at the wavelength of 543 nm as well as a 5-mW laser diode at the wavelength of 635 nm. Using the He-Ne laser, we have measured the displacement with the least count of 68 nm without using an analog to digital converter (ADC). However, when an ADC is used to resolve the intensity profile of the fringe pattern, the displacement or amplitude of the vibration with the accuracy of picometers would be possible. But it requires overcoming the factors producing noise, for example, temperature fluctuation and electromagnetic interference.

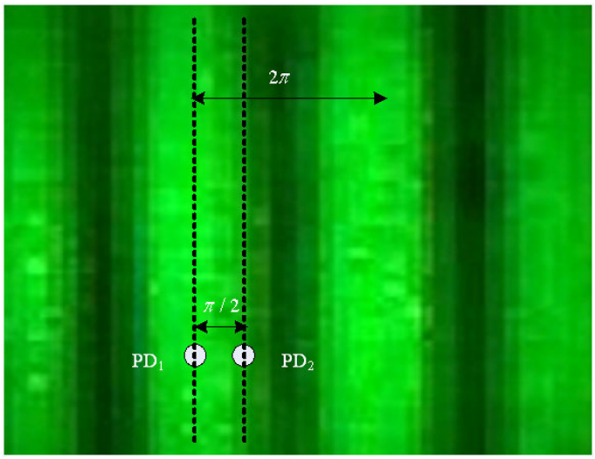

Fig. 2 Two photodiodes, PD_1 and PD_2, spatially separated by $\varphi=\pi/2$ with respect to the intensity prifile of the fringes.

3. Modeling

The block diagram of the processing sequence using analog electronics is shown in Fig. 3. The instantaneous intensity of the moving fringes is sensed by the two photodiodes spatially separated by $\pi/2$. The two signals are then amplified using amplifiers Amp_1 and Amp_2. For analog processing, the direct current (DC) components in the outputs of amplifiers must be removed to make the signal purely sinusoidal oscillating equally between positive and negative peak values. The band-pass filters BPF_1 and BPF_2 are used to remove the DC components as well as the high frequency noise. The circuit similar to the differentiator is used for band-pass filtering (the characteristics of the circuit

is described in Fig. 4). Since both of the signals undergo same differential operation due to BPF_1 and BPF_2, therefore, the time delay produced by these filters is same and causes no problem for further processing. Normalized outputs of the two band-pass filters S_1 and S_2 can be expressed as

$$S_1(t)=\cos[\alpha(t)], \tag{5}$$

$$S_2(t)=\cos[\alpha(t)+\varphi]. \tag{6}$$

Using (3), we have

$$S_2(t)=\mp\sin[\alpha(t)]. \tag{7}$$

When $S_1(t)$ passes through the differentiator (Diff), the output is

$$\frac{dS_1(t)}{dt}=-\frac{dL_1}{dt}\sin[\alpha(t)]. \tag{8}$$

To discriminate the direction a or b of the fringe movement, the two signals from BPF_2 and Diff are multiplied in real time using IC AD633. The output of the multiplier that can be used to discriminate the direction a or b can be expressed as

$$\left[\frac{dS_1(t)}{dt}\right]\left[S_2(t)\right]=\pm\frac{dL_1}{dt}\sin^2\left[\alpha(t)\right]. \tag{9}$$

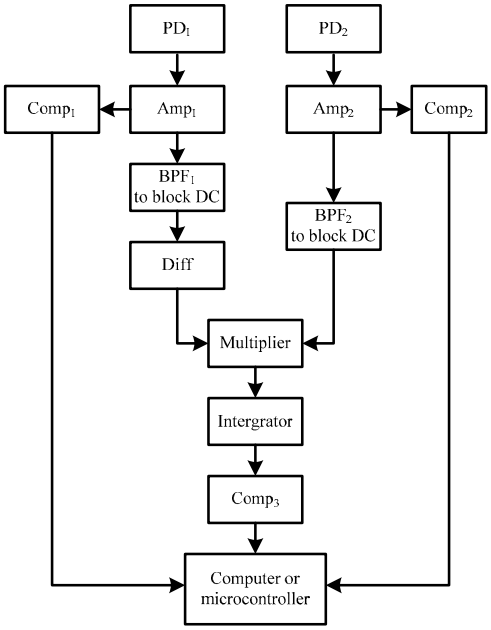

Fig. 3 Processing sequence in analog electronics.

The output of the multiplier will oscillate either in the positive region for direction a or in the negative region for direction b. The direction is indicated by plus and minus signs of dL_1/dt. To remove the oscillations presented in the output of the multiplier for the direction a or b, we have used an electronic integrator. To achieve a clean step function response for the direction of the motion, the output of the integrator passes through a comparator $Comp_3$. To measure the frequency of the vibration, the output of $Comp_3$ is processed via the computer (using LabVIEW) as well as the microcontroller.

Figure 4 is the Bode diagram showing the circuit characteristics of the differentiator. Band-pass filters have the similar characteristics because the circuit is same. The differentiator works well for the vibration with the amplitude of few micrometers and the frequency between 50 Hz and 500 Hz. For example, if the mechanical vibration has an amplitude of 5 μm and a frequency of 50 Hz, then, the frequency of the modulated output of the interferometer would be about 2 kHz. Figure 4(a) shows that the gain of the differentiator is about 10 dB, and Fig. 4(b) shows that the phase difference is less than 30° (90°–60°) at 2 kHz which is tolerable for analog processing proposed in our technique. The complete circuit used for analog processing in our technique is shown in Fig. 5.

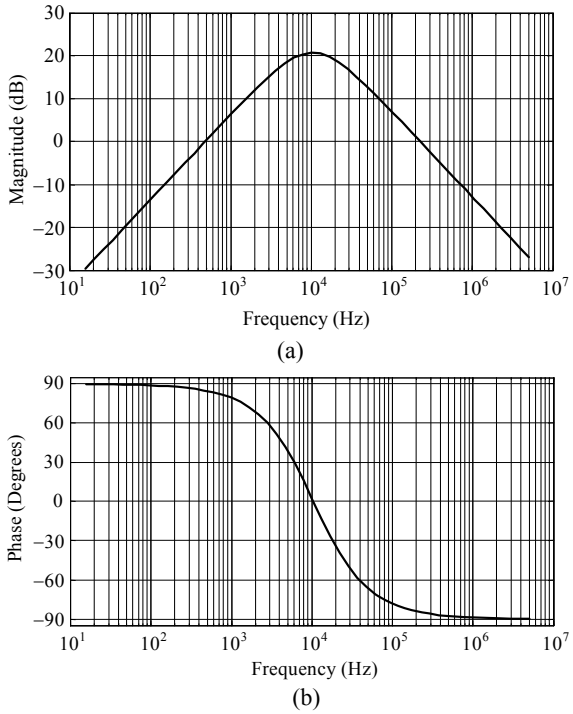

Fig. 4 Bode diagram showing characteristics of the differentiator: (a) the magnitude curve and (b) the phase curve.

The integrator introduces a delay in processing after the output of the multiplier changes its polarity. Simple analysis reveals that the time delay introduced by the integrator is about 1 ms at the frequency of 2 kHz. This delay is equal for each half cycle, therefore, it does not produce error in the measurement. The effects of the differentiator and integrator can be seen from experimental results in Section 4.

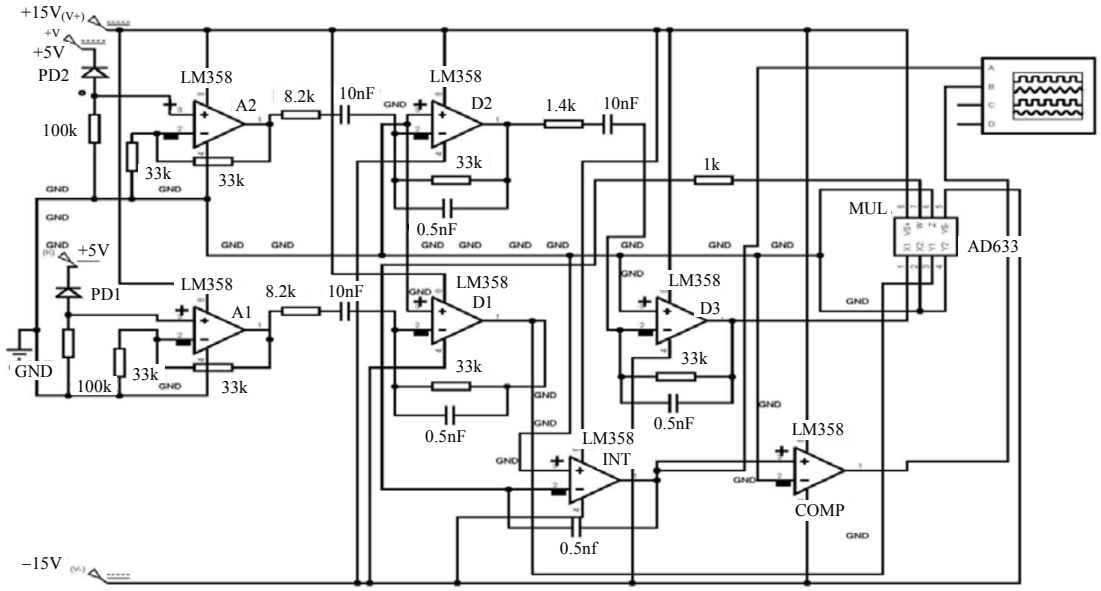

Fig. 5 Electronics circuit for analog processing.

4. Experimental results

Experimental outputs for damped vibrations, at different stages of the analog processing, recorded by the oscilloscope, are shown in Figs. 6(a)–6(d) and 7. The results are in well agreement with (9). It means that the output of the multiplier is either positive or negative depending on the direction of the motion of the vibrating surface. The sign of "±" in (9) shows the direction towards "a" or "b". In Fig. 6(a), it can be noted that outputs of the differentiators 2 and 3 become in and out of phase, respectively during each subsequent half cycle of the vibration. Similarly in Fig. 6(b), the output of the multiplier oscillates subsequently in positive and negative regions. Figure 6(d) shows the output of the system for the damped amplitude of the vibration with a frequency of 200 Hz. The frequency is selected by varying the length of the supporting rod (on the hit and trial basis) on which the mirror M_2 is mounted. The vibration is actuated by providing the impulse force by hitting the supporting rod of M_2. Also, we have confirmed the frequency measured by our system by applying the known frequency through a speaker actuated by a function generator. The mirror M_2 is attached with the diaphragm of the speaker. It can be noted that the number of fringes in one half cycle gives the amplitude of the vibration cycle, and the step function response (high or low) gives real-time information about the direction of the motion. Since the oscillation given to the mirror M_2 is damped, therefore, the oscilloscope captures different data at different time.

It should be noted that the two signals shown in Fig. 6(a) are not perfectly in or out of phase in each half cycle. This error is due to the phase difference introduced by the electronic differentiator Diff, as shown in Fig. 4(b). Another reason of the error is that the two photodiodes, used in our experiment, are not perfectly separated by $\pi/2$, and the sensitive area of the photodiodes is not small enough. The unwanted delay in analog processing can be

compensated by use of the additional circuit but it will increase the complexity of the system. Figure 6(c) shows that the delay introduced by the integrator is about 1 ms.

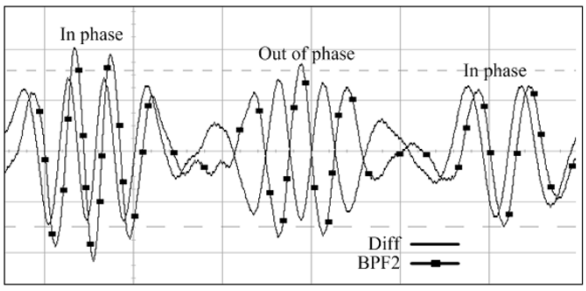

(a)

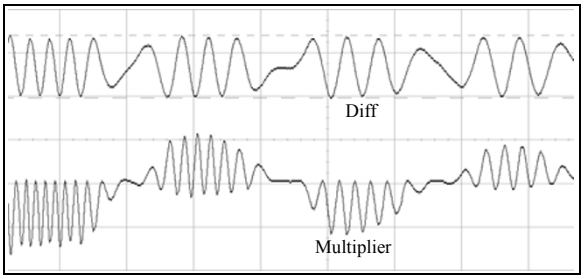

(b)

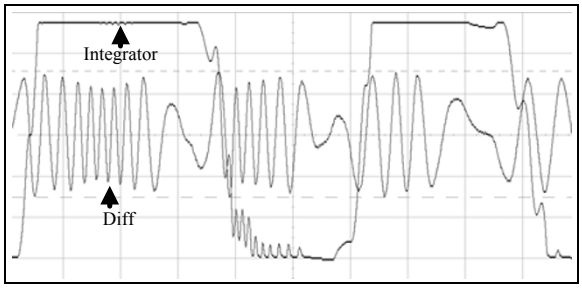

(c)

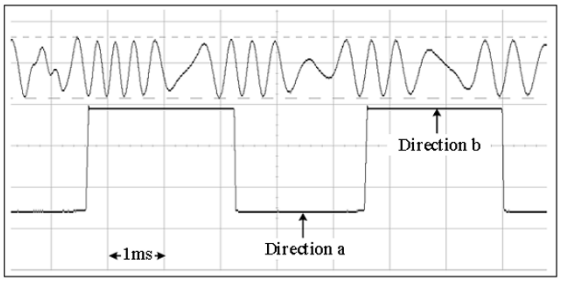

(d)

Fig. 6 Experimental outputs at different stages: (a) BPF_2 and Diff, (b) Diff and multiplier, (c) Diff and integrator, and (d) Diff and $Comp_3$.

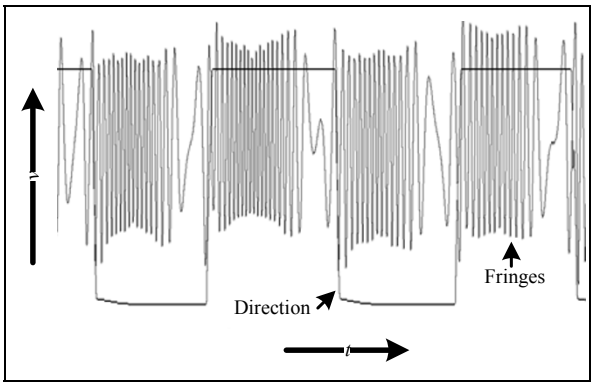

Fig. 7 Final experimental outputs give the frequency and amplitude of the vibration.

5. Conclusions

This paper proposes a new method by which the moving direction of a vibrating surface is detected by the output signal of the step function which is produced with the simple electronic circuit from the interference signal. We have measured mechanical vibrations having magnitude less than 100 nm and frequency in the range of 50 Hz to 500 Hz. Most of the processing is performed in analog electronics. The main advantage of our technique is that the direction of the motion can be detected without computer processing which makes the technique faster. Another merit of the technique, unlike holography, is that the surface under study needs not to be fixed at any point for reference. There are two limitations of the technique. Firstly, the surface under consideration should be reflective and flat. Secondly, modes of the vibration of the whole surface cannot be obtained.

A good application of our proposed technique is the measurement of the amplitude and the frequency of vibrations in the walls of nuclear reactors or other sophisticated buildings. Other applications of our technique are damage detection in materials and recognition of wear and tear in parts of machines.

Acknowledgment

We are grateful to Dr. Masroor Ikram (PIEAS, Pakistan) and all the reviewers of this paper for their valuable comments and suggestions.

References

[1] C. M. Vest and D. W. Sweeney, "Measurement of vibrational amplitude by modulation of projected fringes," *Applied Optics*, vol. 11, no. 2, pp. 449–454, 1972.

[2] B. Koyuncu and J. Cookson, "Semi-automatic measurements of small high-frequency vibrations using time averaged electronic speckle pattern interferometry," *Journal Physics E: Scientific Instruments*, vol. 13, no. 12, pp. 206–208, 1980.

[3] S. Prakash, I. P. Singh, and C. Shakher, "Display of tilt information of vibrating object in time average mode using lateral shearing interferometry and interferometric grating," *Optics and Laser Technology*, vol. 33, no. 2, pp. 117–120, 2001.

[4] L. Yuan, "Recent progress of in-fiber integrated interferometers," *Photonic Sensors*, vol. 1, no. 1, pp. 1–5, 2011.

[5] K. Weir, W. J. O. Boyle, B. T. Meggitt, A. W. Palmer, and K. T. V. Grattan, "A novel adaptation of the Michelson interferometer for the measurement of vibration," *Journal of Lightwave Technology*, vol. 10, no. 5, pp. 700–703, 1992.

[6] R. R. Boullosa and A. P. Lopez, "A simple measurement system for vibrations at low amplitudes," *Applied Acoustics*, vol. 52, no. 2, pp. 155–163, 1997.

[7] Y. Rao, "Study on fiber-optic low-coherence interferometric and fiber Bragg grating sensors," *Photonic Sensors*, vol. 1, no. 4, pp. 382–400, 2011.

[8] C. Shakher, A. L. Vyas, and A. Seth, "Real time monitoring of vibrations using interferometric sensor," in *Proc. ICICS 97*, Singapore, Sept. 9–12, vol. 2, pp. 1185–1188, 1997.

[9] D. H. S. Ding, L. G. Tong, and G. H. Chen, "A sensitive and stable confocal Fabry-Perot interferometer for surface ultrasonic vibration detection," *Chinese Physics*, vol. 10, no. 8, pp. 730–734, 2001.

[10] Y. Jiang and W. Ding, "Recent developments in fiber optic spectral white-light interferometry," *Photonic Sensors*, vol. 1, no. 1, pp. 62–71, 2011.

[11] A. J. Moore, R. McBride, J. S. Barton, and J. D. C. Jones, "Closed-loop phase stepping in a calibrated fiber-optic fringe projector for shape measurement," *Applied Optics*, vol. 41, no. 16, pp. 3348–3354, 2002.

[12] T. K. Gangopadhay, "Non-contact vibration measurement based on an extrinsic Fabry-Perot interferometer implemented using arrays of single-mode fibers," *Measurement Science Technology*, vol. 15, no. 5, pp. 911–917, 2004.

[13] J. A. Garcia-Souto and H. Lamela-Rivera, "High resolution (<1 nm) interferometric fiber-optic sensor of vibrations in high-power transformers," *Optical Express*, vol. 14, no. 21, pp. 9679–9686, 2006.

[14] L. Yuan and Y. Dong, "Loop topology based white light interferometric fiber optic sensor network for application of perimeter security," *Photonic Sensors*, vol. 1, no. 3, pp. 260–267, 2011.

[15] Q. Yu and X. Zhou, "Pressure sensor based on the fiber optic extrinsic Fabry-Perot interferometer," *Photonic Sensors*, vol. 1, no. 1, pp. 72–83, 2011.

[16] G. Siegmund, "Sources of measurement error in laser Doppler vibrometers and proposal for unified specifications," in *Proc. SPIE*, vol. 7098, pp. 70980Y-1–70980Y-13, 2008.